

# Photochromic reactions of reversible coordination of perfluorothionaphthyl radical with flat Ni(II) dithiolate complexes

D.Yu. Vorobyev<sup>a</sup>, V.F. Plyusnin<sup>a,\*</sup>, Yu.V. Ivanov<sup>a</sup>,  
V.P. Grivin<sup>a</sup>, S.V. Larionov<sup>b</sup>, H. Lemmetyinen<sup>c</sup>

<sup>a</sup> Institute of Chemical Kinetics and Combustion, 630090 Novosibirsk, Russia

<sup>b</sup> Institute of Inorganic Chemistry, 630090 Novosibirsk, Russia

<sup>c</sup> Institute of Materials Chemistry, Tampere University of Technology, P.O. Box 589, 33101 Tampere, Finland

Received 11 April 2001; received in revised form 10 October 2001; accepted 26 November 2001

## Abstract

The solutions of perfluoronaphthyl disulfide ((SC<sub>10</sub>F<sub>7</sub>)<sub>2</sub> = (SNF)<sub>2</sub>) and flat 1,1'-dithiolate complexes Ni(II) (NiL<sub>2</sub>) in acetonitrile are shown to be photochromic systems. Absorption of the light pulse of an XeCl excimer laser (308 nm) by these solutions gives new absorption in the visible spectrum region which disappears in a millisecond time domain and the system returns to its original state. The cycle of phototransformations can be repeated many times without degradation of spectral changes in the solution. In the first stage, an excited disulfide molecule dissociates into two perfluorothionaphthyl radicals ( $\bullet$ SC<sub>10</sub>F<sub>7</sub>  $\equiv$   $\bullet$ SNF). These radicals coordinate at almost diffusion rate constant with NiL<sub>2</sub> complexes to form the (SNF) $\bullet$ NiL<sub>2</sub> radical complexes to which this new absorption belongs. The (SNF) $\bullet$ NiL<sub>2</sub> complexes disappear due to dissociation resulting in a free  $\bullet$ SNF radical that either transforms into disulfide upon recombination or reacts again with the initial NiL<sub>2</sub> complex. The optical spectra of intermediates and the rate constants of all transformation stages of these species have been determined. © 2002 Elsevier Science B.V. All rights reserved.

**Keywords:** Photochromic system; Perfluoronaphthyl disulfide; Dithiolate Ni(II) complexes; Laser flash photolysis; XeCl

## 1. Introduction

The photochromism of many organic and inorganic systems has long been known [1,2]. Photochromic materials have been the focus of attention for the last few years because of a practical need for the creation of the systems of reverse optical record of information and light energy accumulation, photochemical switches for optical computers and the development of enzymes with optical switching, etc. The demand for photosensitive materials overlapping a wide range in the UV and visible spectrum regions is extremely high. Therefore, it is highly interesting to discover new photochromic systems and to study the mechanisms of photochemical and dark transformations for them. Natural processes involve numerous proteins and enzymes that reversibly bind substrates for transporting them to certain regions of animal organism and plants. This can be demonstrated by hemoglobin which, in the active center, has a flat coordination unit with an iron ion reversibly adding the oxygen molecule. The reversibility of substrate addition to flat coordination com-

pounds can be used to create new photochromic systems. The appearance of a particle-substrate should be related to a photochemical reaction. Convenient objects, in this case, are the organic peroxides and disulfides with –O–O– and –S–S– bonds which have low energies and can dissociate under the action of light quanta in the blue and nearest UV regions of the spectrum. Disulfides are most attractive because they exhibit strong absorption in the UV region with “tails” stretching to the blue spectrum region. In addition, the disulfide dissociation results in non-active sulfur-centered radicals disappearing upon recombination. In this stage, the 1,1'-dithiolate Ni(II) complexes were chosen as flat coordination compounds because they reversibly coordinate some organic molecules such as pyridines [3–9]. There was sense in assuming that the sulfur-containing radicals can be reversibly built in the coordination sphere of a nickel complex at a great rate constant. The great rate constant is necessary for successful competition with recombination of these radicals occurring with almost diffusion rate constant [10].

Indeed, we have recently established [11,12] that the solutions of thiuramdisulfide (tds  $\equiv$  R<sub>2</sub>NC(S)S–S(S)CNR<sub>2</sub>, where R are the alkyl groups) and flat dithiocarbamate complex of divalent nickel (Ni(dtc)<sub>2</sub>) (ligand dtc<sup>–</sup>  $\equiv$  S<sub>2</sub>CNR<sub>2</sub>)

\* Corresponding author. Tel.: +7-3832-332385; fax: +7-3832-342350.  
E-mail address: plyusnin@ns.kinetics.nsc.ru (V.F. Plyusnin).

display photochromic properties and endure a great number of transformation cycles. Using laser flash photolysis, we have shown that the excited thiuramdisulfide molecule dissociates into two dithiocarbamate radicals ( $\text{dtc}^{\bullet} \equiv \text{S}_2\text{CNR}_2$ ) in the first stage of these transformations. These radicals coordinate with a rate constant close to the diffusion one, with  $\text{Ni}(\text{dtc})_2$  to form the  $(\text{dtc}^{\bullet})\text{Ni}(\text{dtc})_2$  radical complex which has a wide absorption band with a maximum at 400 nm with a “tail” up to 700 nm. The  $(\text{dtc}^{\bullet})\text{Ni}(\text{dtc})_2$  complex dissociates during about 7 ms thus “releasing” the  $\text{dtc}^{\bullet}$  radical which then either transforms into thiuramdisulfide upon recombination or reacts again with the initial  $\text{Ni}(\text{dtc})_2$  complex to form  $(\text{dtc}^{\bullet})\text{Ni}(\text{dtc})_2$ . The repeated radical coordination increases the observed lifetime of radical complex by three orders of magnitude so that absorption vanishes in the second time domains. Thus, the flat  $\text{Ni}(\text{dtc})_2$  complex is an excellent trap for the S-radical. Under standard conditions, the radical vanishes after laser pulse due to recombination during several microseconds and coordination increases its lifetime by six orders of magnitude. Therefore, the solutions disulfide and flat Ni(II) complex are of interest not only for their photochromic properties but also as the systems which repeatedly increase the lifetime of short-lived active radicals.

This paper studies the photochromic transformations of perfluoronaphthyl disulfide ( $(\text{SC}_{10}\text{F}_7)_2$ ) and flat 1,1'-dithiolate Ni(II) complexes ( $\text{NiL}_2$ ) in acetonitrile. The choice of disulfide was determined by the known optical spectrum of  $\bullet\text{SC}_{10}\text{F}_7$  radical [10]. The type of chosen Ni(II) complexes was related to the spectral peculiarities of the complexes and the known geometry, i.e., the flat coordination unit consisting of four sulfur atoms with a central ion of divalent nickel.

## 2. Experimental details

The laser flash photolysis of solutions was carried out on a set-up with an XeCl excimer laser (308 nm, 15 ns, 50 mJ, beam area  $10\text{ mm}^2$ ). For details see Ref. [13]. The exciting and probing light beams fell on a cuvette (thickness varying from 0.1 to 10 mm) at a small angle ( $\sim 2^\circ$ ). When necessary, the cuvette was placed in a quartz optical cryostat blown through with a stream of cold nitrogen in order to vary temperature within a wide range. The temperature was controlled automatically to within  $0.5^\circ\text{C}$ . In some experiments, we used a similar set-up for laser flash photolysis [14] with perpendicular exciting and probing light beams. The photomultiplier signal was recorded on a digital oscilloscope Tektronix 7912AD connected to an IBM computer.

The optical absorption spectra were recorded on spectrophotometers Shimadzu UV-2501, Specord UV-Vis and Specord M40 (Carl Zeiss). Solutions were prepared from the spectrally pure solvents. The intensity of laser pulses was measured by the value of the optical density of anthracene triplet-triplet absorption in the oxygen-free benzene

solution at 431 nm (quantum yield of the triplet state being 0.53, and absorption coefficient of T-T absorption band being  $42\,000\text{ M}^{-1}\text{ cm}^{-1}$  [15]). To remove oxygen, solutions were blown through with nitrogen during 30 min. In the numerical calculations of the kinetics of intermediate optical absorption appearance and decay, the differential equations were solved by a special program and fourth-order Runge-Kutta method.

Perfluoro-2,2'-dinaphthyl disulfide ( $(\text{SC}_{10}\text{F}_7)_2 = (\text{SNF})_2$ ) was obtained by applying bromine to a corresponding thiophenol in acetic acid [16]: m.p.  $116\text{--}117^\circ\text{C}$ . Found: MW = 569.9226,  $\text{C}_{20}\text{F}_{14}\text{S}_2$ . Calculated: MW = 569.9218.  $^{19}\text{F}$  NMR ( $\delta$ , ppm, internal  $\text{C}_6\text{F}_6$ ): 54.2 (dd, peri  $J_{18} = 70\text{ Hz}$ ,  $J_{15} = 18.3\text{ Hz}$ , 1F), 32.5 (d,  $J_{38} = 17\text{ Hz}$ , 3F), 19.8 (dt, peri  $J_{18} = 70\text{ Hz}$ ,  $J_{38} = 17\text{ Hz}$ ,  $J_{48} = 17\text{ Hz}$ , 8F), 17.1 (dt, peri  $J_{45} = 59\text{ Hz}$ ,  $J_{47} = 17\text{ Hz}$ ,  $J_{48} = 17\text{ Hz}$ , 4F), 15.9 (dt, peri  $J_{45} = 59\text{ Hz}$ ,  $J_{15} = 18.3\text{ Hz}$ ,  $J_{56} = 18.5\text{ Hz}$ , 5F), 11.9 (t,  $J_{56} = 18.5\text{ Hz}$ ,  $J_{67} = 18.3\text{ Hz}$ , 6F), 8.1 (t,  $J_{47} = 17\text{ Hz}$ ,  $J_{67} = 18.3\text{ Hz}$ , 7F). The signals of all fluorine nuclei contain not identified extra splitting about 4–2 Hz. Signals assignment in  $^{19}\text{F}$  NMR spectrum was made on the base of fine structure analysis and comparison with  $^{19}\text{F}$  NMR spectrum of 2-mercaptoheptafluoro-naphthalene [17].

## 3. Results and discussion

### 3.1. Flash photolysis of $(\text{SNF})_2$ disulfide: the optical spectrum of $\bullet\text{SNF}$ radical

Fig. 1 shows the optical spectrum of  $(\text{SNF})_2$  disulfide in acetonitrile. A characteristic feature of this disulfide is a long-wave absorption band with a maximum at 350 nm ( $\epsilon = 10\,300\text{ M}^{-1}\text{ cm}^{-1}$ ). In the far UV spectrum region there are even stronger absorption bands with maxima at 216 and 243 nm ( $\epsilon = 61\,400$  and  $47\,100\text{ M}^{-1}\text{ cm}^{-1}$ , respectively). At the wavelength of laser radiation (308 nm) the absorption

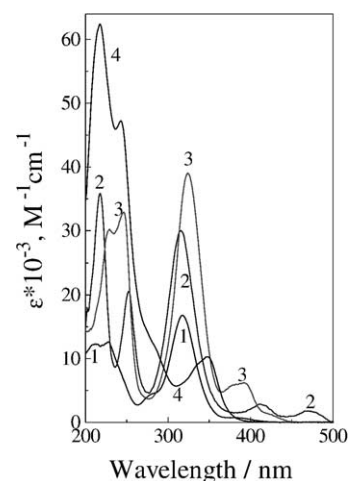


Fig. 1. The optical spectra of the  $\text{Ni}(\text{Et-dtp})_2$  (1),  $\text{Ni}(\text{Et-xan})_2$  (2),  $\text{Ni}(\text{Pr-dtc})_2$  (3) complexes and the  $(\text{SNF})_2$  disulfide (4) in acetonitrile.

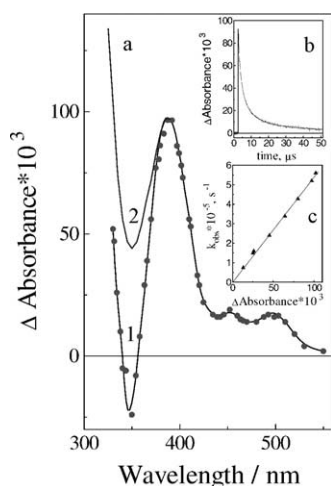


Fig. 2. The optical spectrum of  $\bullet$ SNF radical (a) arising upon laser flash photolysis of  $(\text{SNF})_2$  disulfide solution in acetonitrile (295 K). The insets show the kinetics of the disappearance of radical absorption at 390 nm (b) and the linear dependence of  $k_{\text{obs}}$  for this kinetics upon the treatment by the second-order kinetic law on the value of signal (c).

coefficient is great enough ( $\varepsilon = 5700 \text{ M}^{-1} \text{ cm}^{-1}$ ). The long stationary irradiation of  $(\text{SNF})_2$  solutions in many solvents (methanol, acetonitrile, benzene, etc.) failed to cause any changes in the optical spectrum. However, using laser flash photolysis, one can record intermediate absorption vanishing within a microsecond time domain.

Under irradiation of organic disulfides in the UV spectrum region, the primary process is the break of S–S bond ( $\sim 100 \text{ kJ/mol}$ ) resulting in two sulfur-centered radicals [18–21] (the quantum energy of an XeCl laser at 308 nm being  $400 \text{ kJ/mol}$ ). The absence of spectral changes even under long stationary irradiation of solutions with and without oxygen testifies to a weak chemical activity of S-radical vanishing upon recombination.

Absorption belonging to the perfluorothionaphthyl ( $\bullet$ SNF) radical arises in acetonitrile (Fig. 2a, spectrum 1) after the laser pulse in the perfluorodiphthyl disulfide ( $(\text{SNF})_2$ ) solution. The bleaching observed at 350 nm as a deep gap is assigned to the disappearance of disulfide  $(\text{SNF})_2$  whose absorption band has a maximum at this wavelength (Fig. 1). The absorption coefficient of  $\bullet$ SNF radical absorption band was determined in [10] which allowed us to calculate the corrected spectrum (Fig. 2a, spectrum 2). Thus, in acetonitrile in the 300–600 nm region, this radical is characterized by three absorption bands with maxima at 390, 450 and 490 nm ( $\varepsilon = 7600, 1350$  and  $1400 \text{ M}^{-1} \text{ cm}^{-1}$ , respectively). The spectrum of this radical can be obtained by the flash photolysis of  $\text{SNF}^-$  ion solution in the presence of  $\text{CCl}_4$  as an electron acceptor [10]. The  $\bullet$ SNF radical vanished upon recombination. Therefore, the kinetics of a decrease in the absorption intensity of this particle obeys the second-order kinetic law (Fig. 2b) as in the case of photolysis of both disulfide  $(\text{SNF})_2$  and  $\text{SNF}^-$  ion solution. The linear dependence of observed rate constant ( $k_{\text{obs}}$ ) on

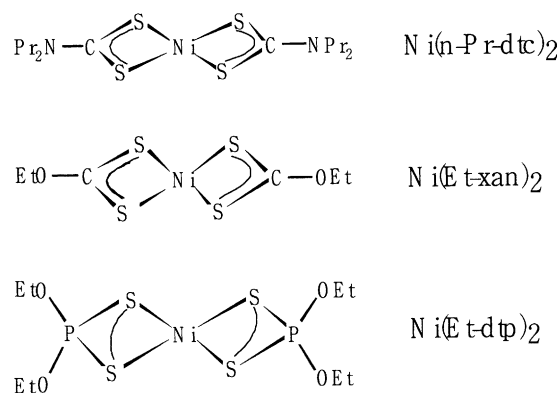


Fig. 3. The structure of dithiolate  $\text{NiL}_2$  complexes.

signal amplitude with zero cut off in the ordinate (Fig. 2c) indicates that the first- or pseudofirst-order contribution to the process of radical disappearance does not exceed  $10^3 \text{ s}^{-1}$  for the usual values  $k_{\text{obs}} \sim 10^5 \text{ s}^{-1}$ . The kinetics of absorption disappearance is independent of oxygen content in the solution which testifies to the absence of reaction between  $\bullet$ SNF radical and oxygen. This is typical of other S-radicals as well [22–24].

### 3.2. The reaction between perfluorothionaphthyl radical and flat Ni(II) complexes: the spectra and kinetic characteristics of the resulting $(\text{SNF})\bullet\text{NiL}_2$ radical complexes

Fig. 3 shows the structure of divalent nickel complexes used to capture the  $\bullet$ SNF radical. The coordination  $\text{NiS}_4$  unit is flat for all three types of the complexes [25–29]. In all complexes, the Ni–S distance is close to  $2.2 \text{ \AA}$ . The optical spectra of these complexes are characterized by strong absorption bands in the UV spectrum region (Fig. 1). All complexes display the charge transfer band in the range 316–325 nm and the deep gap in the range 280–300 nm. This gap provides the access of laser quanta to the disulfide molecule for S-radical generation. In the far UV region, there is the splitted strong absorption band for these complexes. In the visible region, the weaker bands are located to which the d–d transition can contribute. The assignment of the absorption bands of these complexes is given in Refs. [30–32]. The similarity of the optical spectra of these complexes is determined by the same flat coordination  $\text{NiS}_4$  unit and the S–C–S or S–P–S fragments in each ligand.

No photochemical activity is observed in the solutions of these complexes in acetonitrile. The long stationary photolysis under the radiation of a high-pressure mercury lamp causes no changes in the spectra of solutions and no intermediate absorption is observed in pulse experiments. However, adding the  $(\text{SNF})_2$  disulfide to the solutions of  $\text{NiL}_2$  complexes results in absorption differing from that of  $\bullet$ SNF radical. Fig. 4 shows the optical spectra arising after the laser pulse in the  $(\text{SNF})_2 + \text{Ni}(\text{dtp})_2$  system followed by the

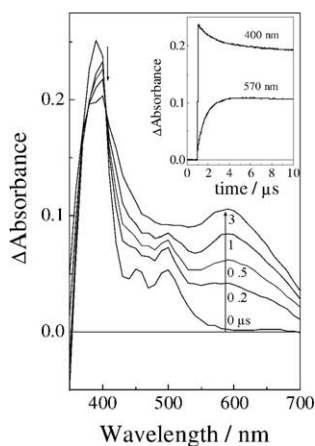


Fig. 4. Intermediate optical spectra arising after the laser pulse of the  $(\text{SNF})_2$  ( $1.6 \times 10^{-4} \text{ M}$ ) +  $\text{Ni}(\text{dtp})_2$  ( $1.3 \times 10^{-4} \text{ M}$ ) system in acetonitrile: (1–5) the spectra taken 0, 0.2, 0.5, 1 and 3 ms after the pulse. The cuvette is 1 cm,  $T = 291 \text{ K}$ . The inset shows the typical kinetic curves.

appearance of the  $\bullet\text{SNF}$  radical spectrum which is quickly transformed (with isosbestic points at 372 and 405 nm) into a new spectrum with bands at 390 and 590 nm.

Reaction between the  $\bullet\text{SNF}$  radical and the complex may follow two ways. The first is the electron transfer from the  $\text{Ni}^{2+}(\text{dtp})_2$  complex to the radical which gives a free  $^-\text{SNF}$  ligand and the  $\text{Ni}^{3+}(\text{dtp})_2$  complex. In this case, however, the UV radiation must quickly convert the  $(\text{SNF})_2$  molecule into two free  $^-\text{SNF}$  ligands which in acetonitrile display no photochemical activity. Thus, this mechanism fails to explain the photochromic character of the system with many transformation cycles. The second possible way is the coordination of  $\bullet\text{SNF}$  radical and the formation of a new complex whose dark reactions may lead to the photochromic transformation of the system. In this case, a new nickel complex  $(\text{SNF})\bullet\text{Ni}(\text{dtp})_2$  is formed to which the new optical spectrum belongs:



The nickel ion in this complex is likely to be in the intermediate valent state (between  $\text{Ni}^{2+}$  and  $\text{Ni}^{3+}$ ) due to electron and spin density redistribution between the central ion and the radical. It should be noted that the long-lived metal-complex-radicals are registered in photodissociation of S,S'-dialkyl and S,S'-alkanediyl derivatives of bis(1,2-ethanedithiolato)nickel complexes [33,34].

The long-run irradiation of the  $(\text{SNF})_2 + \text{Ni}(\text{dtp})_2$  solution by laser pulses causes no changes in the optical spectrum of the system. Therefore, the  $(\text{SNF})\bullet\text{Ni}(\text{dtp})_2$  radical complex vanishes due to monomolecular decay with the escape of the free  $\bullet\text{SNF}$  radical into the solvent volume similarly to

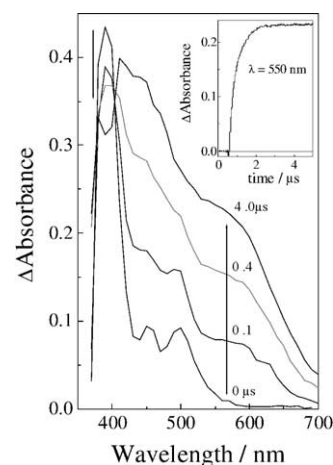


Fig. 5. Intermediate optical spectra arising after the laser pulse of the  $(\text{SNF})_2$  ( $4.7 \times 10^{-4} \text{ M}$ ) +  $\text{Ni}(\text{dte})_2$  ( $1.9 \times 10^{-4} \text{ M}$ ) system in acetonitrile: (1–4) the spectra taken 0, 0.1, 0.4 and 4 ms after the pulse. The cuvette is 1 cm,  $T = 291 \text{ K}$ . The inset shows the typical kinetic curves.

the reaction of  $(\text{dte})\bullet\text{Ni}(\text{dte})_2$  complex disappearance [11]. The rate constant of radical complex dissociation is to be determined below. In the volume, the radical can either encounter the complex and coordinate again (reaction (2)) or can vanish upon recombination (reaction (4)) to regenerate disulfide. Similar changes in the optical spectrum after laser pulse were observed for the  $(\text{SNF})_2 + \text{Ni}(\text{dte})_2$  (Fig. 5) and  $(\text{SNF})_2 + \text{Ni}(\text{xan})_2$  (Fig. 6) systems. In all cases, the wide absorption bands arise with maxima at 400 and 500–600 nm. The latter overlap the considerable part of the visible spectrum range.

To calculate the rate constants of the reaction between the radical and the Ni(II) complex, it is necessary to get information on the absorption coefficient of the  $\bullet\text{SNF}$  radical and radical complexes absorption bands. For the radical, the absorption coefficient has been determined in [10]. The

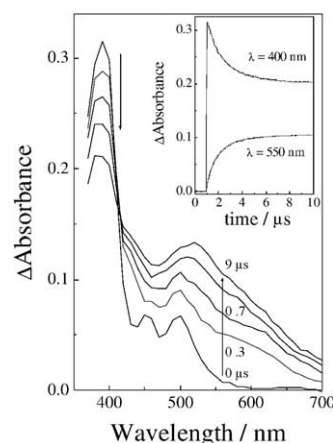


Fig. 6. Intermediate optical spectra arising after the laser pulse of the  $(\text{SNF})_2$  ( $4.2 \times 10^{-4} \text{ M}$ ) +  $\text{Ni}(\text{xan})_2$  ( $7.7 \times 10^{-5} \text{ M}$ ) system in acetonitrile: (1–5) the spectra taken 0, 0.5, 1, 2.5 and 10 ms after the pulse. The cuvette is 1 cm,  $T = 291 \text{ K}$ . The inset shows the typical kinetic curves.

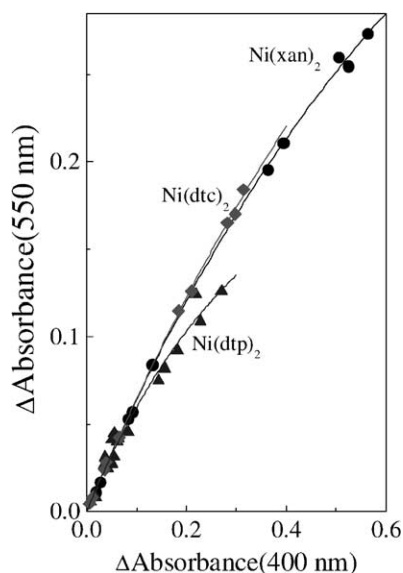


Fig. 7. Determination of absorption coefficients of the (SNF) $\bullet$ NiL<sub>2</sub> radical complexes absorption bands appearing upon flash photolysis of the (SNF)<sub>2</sub> disulfide and NiL<sub>2</sub> complexes in acetonitrile. At 550 nm only the radical complex absorbs. The initial radical concentration was determined from optical density at 400 nm.

absorption coefficient of the radical complex cannot be found from the relationship between the optical densities of the radical and radical complex absorption bands because radical coordination competes with the reaction of recombination. It is necessary to determine the value of radical complex absorption (at 550 nm where the  $\bullet$ SNF radical does not absorb) at times about 10  $\mu$ s (the time of radical complex formation) for the different initial radical concentrations determined by the initial optical density at 400 nm just after the laser pulse. The inclination of the  $\Delta D^{550\text{ nm}} \propto \Delta D^{400\text{ nm}}$  dependence in the region of zero signals will be equal to the ratio between the absorption coefficients of the radical complex and radical. Fig. 7 shows the  $\Delta D^{550\text{ nm}} \propto \Delta D^{400\text{ nm}}$  dependencies for all three nickel complexes (the  $\Delta D^{400\text{ nm}}$  value was varied by changing laser pulse intensity). In the absence of  $\bullet$ SNF radical recombination, the linear dependence would exist even at great  $\Delta D^{400\text{ nm}}$  values. The initial angles of  $\Delta D^{550\text{ nm}} \propto \Delta D^{400\text{ nm}}$  dependencies provided the following values for the absorption coefficients of radical complexes at 550 nm: (SNF) $\bullet$ Ni(dtc)<sub>2</sub>—5200 M<sup>-1</sup> cm<sup>-1</sup>, (SNF) $\bullet$ Ni(dtp)<sub>2</sub>—4900 M<sup>-1</sup> cm<sup>-1</sup> and (SNF) $\bullet$ Ni(xan)<sub>2</sub>—5200 M<sup>-1</sup> cm<sup>-1</sup> (the measurement error being  $\pm 600$  M<sup>-1</sup> cm<sup>-1</sup>). Similar results can be obtained with the absorption coefficient determined from the ratios between optical densities at high concentrations of the initial NiL<sub>2</sub> complex ( $\geq 4 \times 10^{-4}$  M) and much lower radical concentrations ( $\leq 2 \times 10^{-5}$  M), when recombination is almost suppressed.

As follows from Fig. 5, the spectrum of the (SNF) $\bullet$ Ni(dtc)<sub>2</sub> radical complex (the spectrum is taken 4  $\mu$ s after the laser pulse) contains a gap below the 400 nm range caused by

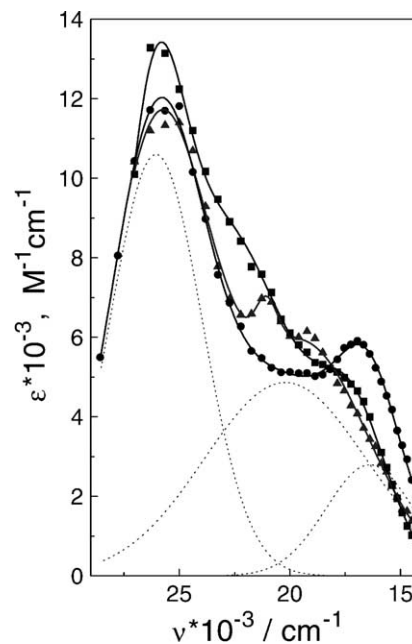


Fig. 8. The corrected optical spectra of (SNF) $\bullet$ NiL<sub>2</sub> radical complexes (with respect to absorption disappearance of the starting NiL<sub>2</sub> complexes). Points—experimental spectra; solid line—description in terms of the sum of three Gaussian components; dotted line—Gaussian components for the spectrum of (SNF) $\bullet$ Ni(dtp)<sub>2</sub> radical complex.

the disappearance of the initial Ni(dtc)<sub>2</sub> complex displaying absorption band at this wavelength (Fig. 1). The available spectra and absorption coefficients of initial complexes make it possible to obtain the corrected spectra of radical complexes (Fig. 8). All (SNF) $\bullet$ NiL<sub>2</sub> complexes have strong absorption bands in the region of 26 000 cm<sup>-1</sup> (385 nm) and about two times weaker bands in the long-wave part of the spectrum 19 000–16 000 cm<sup>-1</sup> (525–625 nm). All spectra are well described by decomposition into three Gaussian components. Fig. 8 demonstrates this decomposition for the (SNF) $\bullet$ Ni(dtp)<sub>2</sub> radical complex (dotted lines). Table 1 summarizes parameters of decomposition into three Gaussian components for all complexes.

The strongest band at 26 000 cm<sup>-1</sup> (385 nm) for the (SNF) $\bullet$ NiL<sub>2</sub> complexes is close in its position and intensity

Table 1  
The spectral parameters of (SNF) $\bullet$ NiL<sub>2</sub> radical complexes in acetonitrile

NiL <sub>2</sub>	$\nu_{\text{max}}$ (cm <sup>-1</sup> )	$\Delta\nu$ (cm <sup>-1</sup> )	$\epsilon$ (M <sup>-1</sup> cm <sup>-1</sup> )
Ni(dtc) <sub>2</sub>	26170	1820	7290
	23200	4630	8820
	17100	2250	3200
Ni(dtp) <sub>2</sub>	26050	2950	10600
	20215	5160	4860
	16390	1880	2800
Ni(xan) <sub>2</sub>	25900	3260	11315
	21070	680	1080
	19290	4020	5720

to the absorption band with a maximum at 390 nm for the free  $\bullet$ SNF radical. The intensity of more long-wave bands is much stronger for complexes than that of similar bands of the free radical. Probably, transitions related to the charge transfer between an ion and a radical contribute to these bands.

The rate constants of  $\bullet$ SNF radical coordination with  $\text{NiL}_2$  complexes can be estimated using the following method. The initial part (5–10%) of the kinetics of absorption appearance at 550 nm of radical complexes (Figs. 4–6) can be treated by the first-order kinetic law and the observed rate constant ( $k_{\text{obs}}$ ) can be obtained which obeys the equation

$$k_{\text{obs}} = \left( \frac{1}{\Delta D_{\infty}} \right) \left( \frac{dD}{dt} \right)_{t=0} = \left( \frac{1}{C_{\infty}} \right) \left( \frac{dC}{dt} \right)_{t=0} \quad (5)$$

where  $\Delta D$  is the value of optical density at 550 nm at the end of radical complex formation,  $C$  the current radical complex concentration and  $C_{\infty}$  the concentration to the end of  $(\text{SNF})\bullet\text{NiL}_2$  formation. According to the scheme of reactions (2)–(4), we get

$$\left( \frac{dC}{dt} \right)_{t=0} = k_1 R_0 [\text{NiL}_2] \quad (6)$$

where  $R_0$  is the initial (after pulse)  $\bullet$ SNF radical concentration and  $[\text{NiL}_2]$  the concentration of the initial Ni(II) complex. Combining these two equations, we get

$$k_{\text{obs}} \left( \frac{C_{\infty}}{R_0} \right) = k_1 [\text{NiL}_2] \quad (7)$$

Thus, the  $k_{\text{obs}} C_{\infty} / R_0$  value should linearly depend on the  $\text{NiL}_2$  concentration with a zero cut off in the ordinate. The inclination determines the bimolecular rate constant of  $\bullet$ SNF radical coordination with  $\text{NiL}_2$  complexes. The  $C_{\infty}$  and  $R_0$  values can be calculated from those for optical densities at 550 and 400 nm, because the absorption coefficients of the radical and radical complexes absorption bands have been determined above. Fig. 9 shows the  $k_{\text{obs}} C_{\infty} / R_0 \propto \text{NiL}_2$  dependence for all three types of the complexes. The linear dependence is observed to be well satisfied. The inclination give the values for coordination rate constants summarized in Table 2. The rate constants are determined to have the same values if the full experimental kinetic curve is fitted to the calculated one obtained by solving the differential equations corresponding to the scheme of reactions (2)–(4).

Coordination rate constants  $k_1$  are close to the diffusion rate constant in acetonitrile ( $k_{\text{diff}} = 8RT/3000\eta = 1.92 \times 10^{10} \text{ M}^{-1} \text{ s}^{-1}$ ) which allows this reaction to successfully

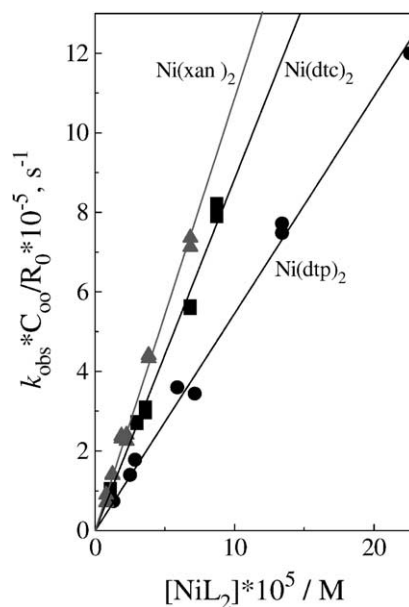


Fig. 9. Determination of bimolecular rate constants of  $\bullet$ SNF radical coordination with  $\text{NiL}_2$  complexes (see text) in acetonitrile.

compete with radical recombination. The greatest rate constant is realized for the  $\text{Ni}(\text{xan})_2$  complex that has the smallest steric obstacles to S-radical approach. The smallest rate constant is typical of  $\text{Ni}(\text{dtp})_2$  which has the groups at the ligand periphery located along the axis perpendicular to the plane of the  $\text{NiS}_4$  coordination unit and protecting this node.

The closeness of coordination rate constant to the diffusion limit indicates the small values of the activation energy of S-radical entrance into the coordination sphere. The temperature dependence of  $k_1$  for all complexes (Fig. 10) and the activation energy (Table 2) have been determined by measuring the kinetics of optical absorption appearance of radical complexes within a wide temperature range (up to 232 K—acetonitrile freezing point). Indeed, the activation energies (7.2–12.8 kJ/mol) are close to that of diffusion in acetonitrile (9.6 kJ/mol). The last value is determined from the temperature dependence of  $k_{\text{diff}}$  ( $k_{\text{diff}} = 8RT/3000\eta$ ) using temperature-dependent acetonitrile viscosity [35]. The values of pre-exponential factors for  $k_1$  are in the range  $(1.6\text{--}9.7) \times 10^{11} \text{ M}^{-1} \text{ s}^{-1}$ .

The reaction kinetics of particles in solvent cage is very complex. It is known that in this case the repeated contacts of species are possible [36,37]. The estimation shows that for the S-radical coordination with a flat Ni(II) complex, a steric

Table 2

The rate constants and activation energy of the coordination of  $\bullet$ SNF radical with  $\text{NiL}_2$  dithiolate complexes ( $k_1$ ,  $E_1$ ) and the decay of  $(\text{SNF})\bullet\text{NiL}_2$  radical complexes ( $k_2$ ,  $E_2$ ) in acetonitrile

$\text{NiL}_2$	$k_1 \times 10^{-9} (\text{M}^{-1} \text{ s}^{-1})$ at 298 K	$\log(k_{10}) (\text{M}^{-1} \text{ s}^{-1})$	$E_1 (\text{kJ M}^{-1})$	$k_2 \times 10^{-5} \text{ s}^{-1}$ at 298 K	$\log(k_{20}) (\text{s}^{-1})$	$E_2 (\text{kJ M}^{-1})$
$\text{Ni}(\text{dtp})_2$	$5.5 \pm 0.1$	$12.0 \pm 0.1$	$12.8 \pm 0.5$	$1.3 \pm 0.1$	$9.0 \pm 0.5$	$23.0 \pm 1.7$
$\text{Ni}(\text{dte})_2$	$8.8 \pm 0.1$	$11.2 \pm 0.1$	$7.2 \pm 0.6$	$0.17 \pm 0.03$	$7.3 \pm 0.5$	$10.9 \pm 1.3$
$\text{Ni}(\text{xan})_2$	$10.8 \pm 0.1$	$11.8 \pm 0.1$	$10.0 \pm 0.5$	$1.0 \pm 0.2$	$6.6 \pm 0.2$	$17.2 \pm 1.7$

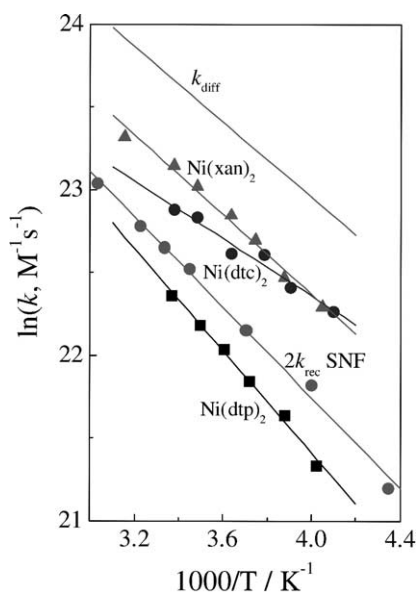


Fig. 10. The dependence of rate constants of  $\bullet$ SNF radical coordination with  $\text{NiL}_2$  complexes and recombination on reverse temperature. The  $k_{\text{diff}}$  value is calculated from the data on the temperature dependence of acetonitrile viscosity from the formula  $k_{\text{diff}} = 8RT/3000\eta$ .

factor (the coordination only by the S atom) can be about 0.01–0.02, and the first contact of particles can be unsuccessful. However, the rotatory diffusion of S-radical between the repeated contacts can give the correct orientation of radical and lead to the reaction. The dithiocarbamate ( $\text{dte}^\bullet$ ) radical has more irregular manifold structure (presence of alkyl groups with nitrogen atom and two sulfur atoms) and its rotatory diffusion is more slow in comparison with the rotatory diffusion of more smooth plain  $\bullet$ SNF radical. This difference in the structure and rate of rotatory diffusion can be the reason of more small rate constant of the dithiocarbamate radical coordination ( $2.5 \times 10^9 \text{ M}^{-1} \text{ s}^{-1}$  [11]) with the  $\text{Ni}(\text{dte})_2$  complex in comparison with the  $\bullet$ SNF radical ( $8.8 \times 10^9 \text{ M}^{-1} \text{ s}^{-1}$ , Table 2).

### 3.3. Reaction of the disappearance of $(\text{SNF})^\bullet\text{NiL}_2$ radical complexes

With the individual lifetime of about 7 ms, the ( $\text{dte}^\bullet$ )  $\text{Ni}(\text{dte})_2$  radical complex vanishes rather slowly due to the repeat coordination of radicals in the second time domain [11]. This allowed one to accumulate the radical complex in the cooled methanol solutions and to record its ESR spectrum [12]. Radical complexes involving  $\bullet$ SNF radical decay much quicker. Fig. 11 shows the kinetics of optical absorption disappearance at 550 nm of the  $(\text{SNF})^\bullet\text{Ni}(\text{dtp})_2$  radical complex in acetonitrile at the different amplitudes of laser pulse (the different initial concentrations of  $\bullet$ SNF radical). The similar kinetic curves have been obtained for the disappearance of other  $(\text{SNF})^\bullet\text{NiL}_2$  radical complexes. Fig. 11 (solid lines) shows the calculated kinetics of radical

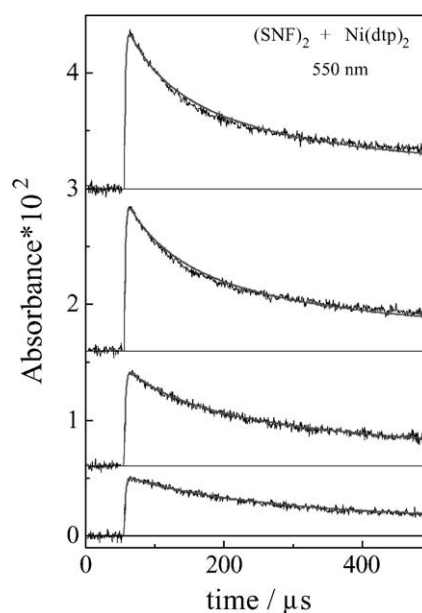


Fig. 11. The kinetics of optical absorption disappearance (550 nm) of the  $(\text{SNF})^\bullet\text{Ni}(\text{dtp})_2$  radical complex in acetonitrile. The kinetics differ in their initial concentrations of  $\bullet$ SNF radical. For convenience, the upper three kinetics are shifted along the ordinate. Solid line—calculation by solving differential equations corresponding to the scheme of reactions (2)–(4).

complex absorption disappearance by solving differential equations by the numerical method (fourth-order Runge–Kutta) which correspond to the schemes of reactions (2)–(4). The  $k_1$  and  $k_3$  constants have been obtained by studying the processes of radical complex formation and radical recombination. Therefore, treating all kinetics, only  $k_2$  was varied. As follows from the figure, the calculated curves are in fair agreement with the experimental ones. These calculations give  $k_2 = (1.3 \pm 0.1) \times 10^5 \text{ s}^{-1}$ . Thus, the  $(\text{SNF})^\bullet\text{Ni}(\text{dtp})_2$  radical complex decomposes during about 7.7  $\mu\text{s}$  and its lifetime is three orders of magnitude shorter than that of the ( $\text{dte}^\bullet$ )  $\text{Ni}(\text{dte})_2$  complex (7.8 ms [11]). The observed lifetime of the  $(\text{SNF})^\bullet\text{Ni}(\text{dtp})_2$  complex increases by about two orders of magnitude up to several hundreds of microseconds due to repeat radical coordination and depends on the initial concentration of the initial  $\text{Ni}(\text{dtp})_2$  complex and the depth of phototransformations (laser pulse intensity).

The considerable difference of the  $k_2$  value for the  $(\text{SNF})^\bullet\text{NiL}_2$  complexes (Table 2) may be due to the intricate reaction kinetics in a solvent cage. In a case of the possible reversible coordination of S-radicals, this kinetics becomes more complicated. When the S-radical leaves the coordination sphere of  $\text{Ni}(\text{II})$  ion, it is located some time with the ion in a solvent cage. The repeated contacts can result to the repeated coordination of the S-radical, which has not yet escaped to solvent bulk. Apparently, the complex dynamics of the radical motion in cage and the features of complex structure, namely the structure of peripheral part of the  $\text{Ni}(\text{dte})_2$  complex (presence of irregular manifold alkyl

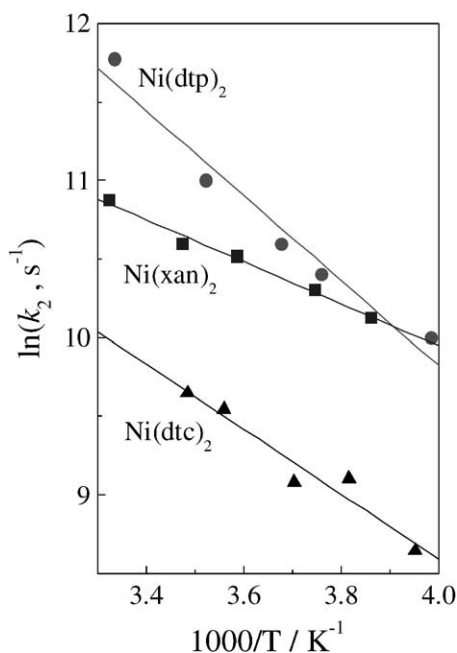


Fig. 12. Dependence of the rate constants of the (SNF) $\bullet$ NiL<sub>2</sub> complexes disappearance on reverse temperature.

groups) result to the rate constants of radical dissociation on one order less than for two other complexes.

Knowing the  $k_1(T)$  and  $k_3(T)$  dependencies (Fig. 10) (measurement of the kinetics of radical complex formation and radical recombination at different temperatures), we have calculated the kinetics of radical complex disappearance, determined the rate constants  $k_2$  within a wide temperature range, and established the activation energy of  $\bullet$ SNF radical dissociation. Fig. 12 shows the  $k_2 \propto 1/T$  dependence for all three types of radical complexes. The activation energy of radical complex decay is shown in Table 2. For (SNF) $\bullet$ Ni(dtp)<sub>2</sub>, the activation energy is 23 kJ/mol. For other two, it is even lower. It is known that the equilibrium constant for the (2)–(3) type reactions is of the form

$$K = \exp\left(\frac{-\Delta G}{RT}\right) = \exp\left(-\frac{\Delta H - T\Delta S}{RT}\right) \\ = \exp\left(\frac{\Delta S}{R}\right) \exp\left(-\left(\frac{\Delta H}{RT}\right)\right)$$

where  $\Delta G$ ,  $\Delta H$  and  $\Delta S$  are the free energy, enthalpy and entropy of radical complex formation, respectively. On the other hand, we get

$$K = \frac{k_2}{k_1} = \left(\frac{k_{20}}{k_{10}}\right) \exp\left(-\frac{E_2 - E_1}{RT}\right)$$

where  $k_1$  and  $k_2$  are the rate constants of direct and reverse reactions, and  $k_{10}$  and  $k_{20}$  are the pre-exponential factors. These relationships show that a change in  $\Delta H$  enthalpy upon radical coordination (actually, the energy of Ni– $\bullet$ SNF bond) is equal to the difference in activation energies and, according to Table 2, for the (SNF) $\bullet$ NiL<sub>2</sub> radical complexes, it is in the range 3.7–10.2 kJ/mol. The small values of S-radical

bond energy account for the short lifetime of these radical complexes.

In these conditions, irradiation in the cooled methanol solutions ( $\sim 175$  K) does not allow one to accumulate radical complex for recording its ESR spectrum. Even for the (SNF) $\bullet$ Ni(dtp)<sub>2</sub> complex (the bond energy being the greatest) at 175 K, the decay takes 10 ms (estimated from the  $k_2$  temperature dependence). The observed time of radical complex disappearance increases at this temperature to fractions of a second. However, solution solidification with decreasing temperature to 109 K (methanol vitrification point) takes several seconds which substantially exceeds the time of radical complex disappearance.

#### 4. Conclusions

The laser flash photolysis has shown that the  $\bullet$ SNF radical with a rate constant close to the diffusion one reversibly coordinates with the flat NiL<sub>2</sub> complexes to form the (SNF) $\bullet$ NiL<sub>2</sub> radical complexes. These particles display strong absorption bands in the visible spectrum range. The lifetime of radical complexes amounts to several microseconds (the lifetime of an individual complex). However, the observed lifetime can reach several hundreds of microseconds owing to repeat radical coordination.

#### Acknowledgements

The financial support of the Russian Foundation for Basic Research (Grant Nos. 99-03-33308 and 99-03-32272), Russian Federal Scientific Program “Integration” (Grant No. 274) and Zamaraev Charitable Scientific Foundation is gratefully acknowledged.

#### References

- [1] H. Durr, H. Bouas-Laurent (Eds.), *Photochromism: Molecules and Systems*, Elsevier, Amsterdam, 1990.
- [2] V.A. Barachevskii, G.I. Lashkov, V.A. Zehomskii, *Photochromism and Its Application*, Khimiya, Moscow, 1977.
- [3] D.R. Dakternieks, D.P. Graddon, *Aust. J. Chem.* 24 (1971) 2509.
- [4] M. Nanjo, T. Yamasaki, *J. Inorg. Nucl. Chem.* 32 (1970) 2411.
- [5] J.R. Angus, G.M. Woltermann, J.R. Wasson, *J. Inorg. Nucl. Chem.* 33 (1971) 3967.
- [6] H.E. Francis, G.L. Tincher, W.F. Wagner, J.R. Wasson, G.M. Woltermann, *Inorg. Chem.* 10 (1971) 2620.
- [7] S.E. Livingstone, A.E. Mihkelson, *Inorg. Chem.* 11 (1970) 2545.
- [8] S. Ooi, Q. Fernando, *Inorg. Chem.* 6 (1967) 1558.
- [9] L. Ang, D.P. Graddon, L.F. Lindoy, S. Prakash, *Aust. J. Chem.* 28 (1975) 1005.
- [10] V.F. Plyusnin, Yu.V. Ivanov, V.P. Grivin, D.Yu. Vorobyev, S.V. Larionov, A.M. Maksimov, V.E. Platonov, N.V. Tkachenko, H. Lemmetyinen, *Chem. Phys. Lett.* 325 (2000) 153.
- [11] Yu.V. Ivanov, V.F. Plyusnin, V.P. Grivin, S.V. Larionov, *J. Photochem. Photobiol. A* 119 (1998) 33.
- [12] Yu.V. Ivanov, V.F. Plyusnin, V.P. Grivin, S.V. Larionov, *Chem. Phys. Lett.* 310 (1999) 252.



- [13] V.P. Grivin, V.F. Plyusnin, I.V. Khmelinski, N.M. Bazhin, M. Mitewa, P.R. Bontchev, *J. Photochem. Photobiol. A* 51 (1990) 371.
- [14] H. Lemmetyinen, R. Ovaskainen, K. Nieminen, K. Vaskonen, I. Sychchikova, *J. Chem. Soc., Perkin Trans. 2* (1992) 113.
- [15] R.H. Compton, T.V. Grattan, T. Morrow, *J. Photochem.* 14 (1980) 61.
- [16] P. Robson, M. Stacey, R. Stephens, J.C. Tatlow, *J. Chem. Soc.* (1960) 4754.
- [17] G.M. Brooke, *J. Fluorine Chem.* 43 (1989) 393.
- [18] D.D. Carlson, A.R. Knight, *Can. J. Chem.* 51 (1973) 1410.
- [19] P.M. Rao, J.A. Copeck, A.R. Knight, *J. Chem.* 45 (1967) 1369.
- [20] K. Sayamol, A.R. Knight, *Can. J. Chem.* 46 (1968) 999.
- [21] P.M. Rao, A.R. Knight, *Can. J. Chem.* 46 (1968) 2462.
- [22] B.M. Aveline, I.E. Kochevar, R.W. Redmont, *J. Am. Chem. Soc.* 117 (1995) 9699.
- [23] B.M. Aveline, I.E. Kochevar, R.W. Redmont, *J. Am. Chem. Soc.* 118 (1996) 10113.
- [24] O. Ito, M. Matsuda, *Can. J. Chem.* 56 (1978) 1080.
- [25] M. Bonamico, G. Dessy, C. Mariani, A. Vaciago, L. Zambonelli, *Acta Crystallogr.* 19 (1965) 619.
- [26] Q. Fernando, C.D. Green, *J. Inorg. Nucl. Chem.* 29 (1967) 647.
- [27] A.I. Prsjazhnyuk, V.K. Belskii, E.V. Kolchinskii, *Koord. Khim.* 13 (1987) 119.
- [28] A.I. Prsjazhnyuk, V.K. Belskii, E.V. Kolchinskii, *Koord. Khim.* 13 (1987) 977.
- [29] Z. Travnicek, R. Pastorek, J. Marek, *Collect. Czech. Chem. Commun.* 59 (1994) 616.
- [30] C.K. Jorgensen, *J. Inorg. Nucl. Chem.* 24 (1962) 1571.
- [31] S.E. Livingstone, R.A. Mihkelson, *Inorg. Chem.* 9 (1970) 2545.
- [32] J.R. Angus, J.R. Wasson, *J. Coord. Chem.* 1 (1971) 309.
- [33] M. Ohtani, S. Ohkoshi, M. Kajitani, T. Akiyama, A. Sugimori, S. Yamauchi, Y. Ohba, M. Iwaizumi, *Inorg. Chem.* 31 (1992) 3873.
- [34] A. Sugimori, *Coord. Chem. Rev.* 159 (1997) 397.
- [35] B.P. Nikolskii (Ed.), *Spravochnik Khimika (Handbook of Chemist)*, Vol. 1, Khimiya, Moscow, 1966, pp. 568–571, 990–1000.
- [36] R.M. Noyes, *Progress in Reaction Kinetics*, Vol. 1, Pergamon Press, New York, 1961 (Chapter 5).
- [37] A.G. Kofman, A.I. Burshtein, *Chem. Phys.* 27 (1978) 217.